PCCP

PAPER

View Article Online
View Journal | View Issue

Cite this: Phys. Chem. Chem. Phys., 2015, **17**, 3482

Behind the color switching in gasochromic VO_2†

Jeng-Lung Chen,[a] Chun-Chieh Chang,[b] Ying-Kai Ho,[bc] Chi Liang Chen,*[b] Chih-Chin Hsu,[a] Wei-Luen Jang,[a] Da-Hua Wei,[c] Chung-Li Dong,*[a] Chih-Wen Pao,[a] Jyh-Fu Lee,[a] Jin-Ming Chen,[a] Jinghua Guo[d] and Maw-Kuen Wu[b]

Received 13th October 2014, Accepted 11th December 2014

DOI: 10.1039/c4cp04623d

www.rsc.org/pccp

Gasochromic VO_2 thin films were fabricated by the sol–gel spin-coating technique. The results of X-ray absorption spectroscopy and resonant inelastic X-ray scattering spectroscopy reveal that the origin of gasochromic coloration in VO_2 is strongly related to the modulation of its structure and the electron–electron correlation. Upon gasochromic coloration, not only does the valence state change with the incorporation of hydrogen, but also the film undergoes the modification of the local atomic structure. The structural distortion varies the strength of hybridization of the O 2p–V 3d states and the bond distance of V–O and V–O varies. In the hydric process, the local atomic structure of VO_2 changes from that of an un-symmetric to that of a symmetric V–O framework. The incorporated hydrogen adds electrons into the V 3d t_{2g} orbital, enhancing the electron–electron correlation by reducing the V–V distance. This work presents a new physical insight in which the modulation of the electron–electron correlation is exploited to control the bleached and colored states, giving rise to the gasochromic phenomenon. The strong correlation among atomic spatial rearrangement, electronic structures, and transmittance supports a cooperative mechanism of the VO_2 gasochromic transition. These results reveal a clear correlation between the dynamics of the lattice structure and the electronic properties and suggest a possible pathway to gasochromism and elucidation of its mechanism.

Introduction

Recently, gasochromic switching thin films have been widely investigated because these thin films are the most promising gas-sensing materials.[1–4] The vanadium oxide system is simple and inexpensive because only a single layer film of this material, covered with a catalyst, suffices to change color. The gasochromic effect, exhibited by WO_3, MoO_3, and V_2O_5, can be exploited in H_2 gas sensor applications.[5] Of particular interest is the vanadium oxide film, which has high transparency, high electrochemical activity and high stability. Among the aforementioned oxides, VO_2 undergoes a metal-insulator transition (MIT) that is not fully understood. Many studies of VO_2 are being carried out to understand the mechanism of the MIT with a view of developing solid-state devices.[6,7] It has been suggested that distortion of the unit-cell and strong electron–lattice coupling cause a Perierls-type MIT and electron–electron correlation gives rise to the Mott–Hubbard-type MIT.[8,9] Above the transition temperature T_{MIT} = 341 K, VO_2 is in the metallic phase with a tetragonal rutile (R) lattice structure, which is transformed to a semiconductor with monoclinic (M) crystal symmetry below T_{MIT}.[10,11] The phase transition drastically changes the electrical and optical properties, making VO_2 an excellent candidate for use in intelligent windows.[12] Thermochromic smart VO_2 has been incorporated into solar cells to form smart windows, which combine energy-saving and electricity generating properties, on account of its phase transition.[13] The VO_2 has different oxide-phases with different crystalline structures, and the stability of films of this material is sensitive to the growth conditions. Recently, several efforts have been made to control T_{MIT} by doping VO_2 in thermochromic devices with metal ions or using various substrates.[14–17] Although doping with tungsten is known to be the most effective method,[18] doping with heavy elements affects transparency. Accordingly, obtaining such a device without heavy doping would be of many values to effective application. In this work, an amorphous VO_2-like thin film is successfully fabricated by the sol–gel process. To the best of our knowledge, this work is the first in which VO_2 is utilized as gasochromic glass.

Advanced technology arises from the understanding of fundamental science, and depends importantly on characterization

[a] National Synchrotron Radiation Research Center, Hsinchu 30076, Taiwan. E-mail: dong.cl@nsrrc.org.tw
[b] Institute of Physics, Academia Sinica, Taipei 11529, Taiwan. E-mail: clchen@phys.sinica.edu.tw
[c] Department of Mechanical Engineering, National Taipei University of Technology, Taipei 10608, Taiwan
[d] Advanced Light Source, Lawrence Berkeley National Laboratory, Berkeley, CA 94720, USA

† Electronic supplementary information (ESI) available. See DOI: 10.1039/c4cp04623d

tools for directly observing both physical and chemical properties. Without knowledge of the fundamental electronic and atomic structures of materials and the changes in their structures upon various reactions, engineering these materials to widen their range of practical applications is difficult. In this work, X-ray absorption spectroscopy (XAS) and resonant inelastic X-ray scattering spectroscopy (RIXS) are utilized to elucidate the electronic properties of VO_2 thin films and explicate the mechanism of its color switching. XAS at the V K- and L-edges reveals the local atomic and electronic structures of mixed-valent vanadium following gasochromism. The incorporation of hydrogen into the coloration interaction is expected to distort the crystal structure, affecting the O–V–O bonding and the unoccupied density of states of 3d orbitals. Extended X-ray absorption fine structure (EXAFS) spectroscopy provides the information on the local atomic structure around the absorbing atoms, including the species and the number of atoms in a particular coordination shell, the interatomic distance and structural disorder. Thus, EXAFS is a powerful tool for studying the local structure of the amorphous materials with a short-range order. The X-ray emission spectrum (XES) probes the de-excitation of the XAS final state and provides information about the ground state of the system that is reached *via* the intermediate excited states, which reflect the local partial density of states (LPDOS). XES is therefore a complementary tool to XAS and the combined absorption–emission spectra yield information about the bandgap. The excitation in XES is resonantly enhanced at particular excitation energies and so is recognized as resonant inelastic X-ray scattering (RIXS).[19] The final state of RIXS has the same symmetry as the initial state of the X-ray absorption process. Therefore, a forbidden electronic transition such as the d–d excitation, which cannot be observed in conventional XAS, can be measured because two dipole transitions are involved. No d–d excitation is expected to be observable in a d^0 system. Such excitation is very sensitive to the occupancy of the 3d shell and electron correlation. The d–d excitations are expected to be evident in the RIXS spectra for the gasochromic VO_2 thin film during its color switching. Most studies on this class of films concern their optical properties. This report elucidates a relevant but rarely utilized means of elucidating the fundamental electronic structure and lays a foundation for engineering better materials.

Experimental

The precursor sol for VO_2 was prepared from vanadium oxide (V_2O_5) powder, in hydrogen peroxide, acetic acid, 95% ethanol and DI-water mix solution. The pre-deposited glass substrate with a dimension of $2.5 \times 2.5 \times 0.12$ cm^3 was spin-coated with the corresponding precursor sol at a speed of 3000 rpm for 20 s. The prepared film (a film thickness of $\sim$180 nm, measured by SEM) was dried at 80 °C for one hour and then annealed at 350 °C for two hours to yield the VO_2 film. The quality of the sample was determined by X-ray powder diffraction (XRD) (Fig. S1, ESI†). A thin layer of catalyst (Pt) was then deposited on the film. The transmittance spectra of the films were obtained using a spectrophotometer (Mini-D2T, Ocean Optics, Inc., USA), with a range of detectable wavelengths from 350 nm to 1700 nm. The V K-edge XAS was recorded in the fluorescence mode using a Lytle detector at beamline BL17C at the National Synchrotron Radiation Research Center (NSRRC),[20] Hsinchu, in Taiwan. All spectra were normalized to unit step height in the absorption coefficient from well below to well above the edges. Pure vanadium metal foil was used for energy calibration. Measurements of XAS and XES at the V $L_{2,3}$-edges and O K-edge were made at beamline 7.0.1 at the Advanced Light Source of Lawrence Berkeley National Laboratory.[21] The XAS spectra were obtained in the total electron yield mode by measuring the sample drain current during the scanning of the photon energy of the incident monochromatic X-ray. The XAS spectra were normalized to the photon current from a clean gold mesh to account for the variations in the intensity of the incident beam, and the energy was calibrated using an NiO single crystal. The XES spectra were recorded using a high-resolution Rowland-mount grazing-incidence grating spectrometer with a two-dimensional detector,[22] and were normalized according to the beam current per unit time. The data were collected *in situ* under a vacuum with a base pressure of lower than 2.7×10^{-9} torr, using a gas cell, to maintain the sample in a hydrogen environment.

Results and discussion

Fig. 1(a) presents the transmission spectra of gasochromic VO_2 films in the bleached and colored states (for a full range of detectable wavelengths, see Fig. S2, ESI†). The transmittance in the colored state differs significantly from that in the bleached state. The transmittance of the film in the colored state to visible light at around 400 nm is approximately 50% lower than that in the bleached state. The optical properties are generally accepted to be correlated with the change in the valence of the vanadium in the film. Fig. 1(b) shows photographs of VO_2 films in the bleached and colored states, which clearly indicate that the color changed from yellow to gray upon exposure to H_2. Fig. 1(c) displays the cross-sectional SEM image of the thin film that was formed by the sol–gel process and deposited on a glass substrate, and the thickness of this film is determined to be about 170 nm. The surface of the film is capped with a thin layer of catalyst (Pt) with a thickness of around 8 nm.

The depth profiles of the concentration of the Pt/VO_2 film were further obtained using a secondary ion mass spectrometer (SIMS). Fig. 1(d) presents the SIMS depth profiles of the O, Si and Pt (from left to right panel) concentrations of the films. The black line and the red line correspond to the films before and after exposure to H_2. The Si intensity increases at the boundary between the glass substrate and the Pt/VO_2 thin film. The small discrepant position at which the Si intensity increases is caused by a small difference in the film thickness. The SIMS depth profile in the middle panel reveals a sharp rise in the Pt concentration close to the surface. Pt dominates the surface of each film and the concentrations at the surfaces of both films are similar. The SIMS depth profile of O demonstrates that the oxygen content in the film is unchanged upon coloration. To determine the

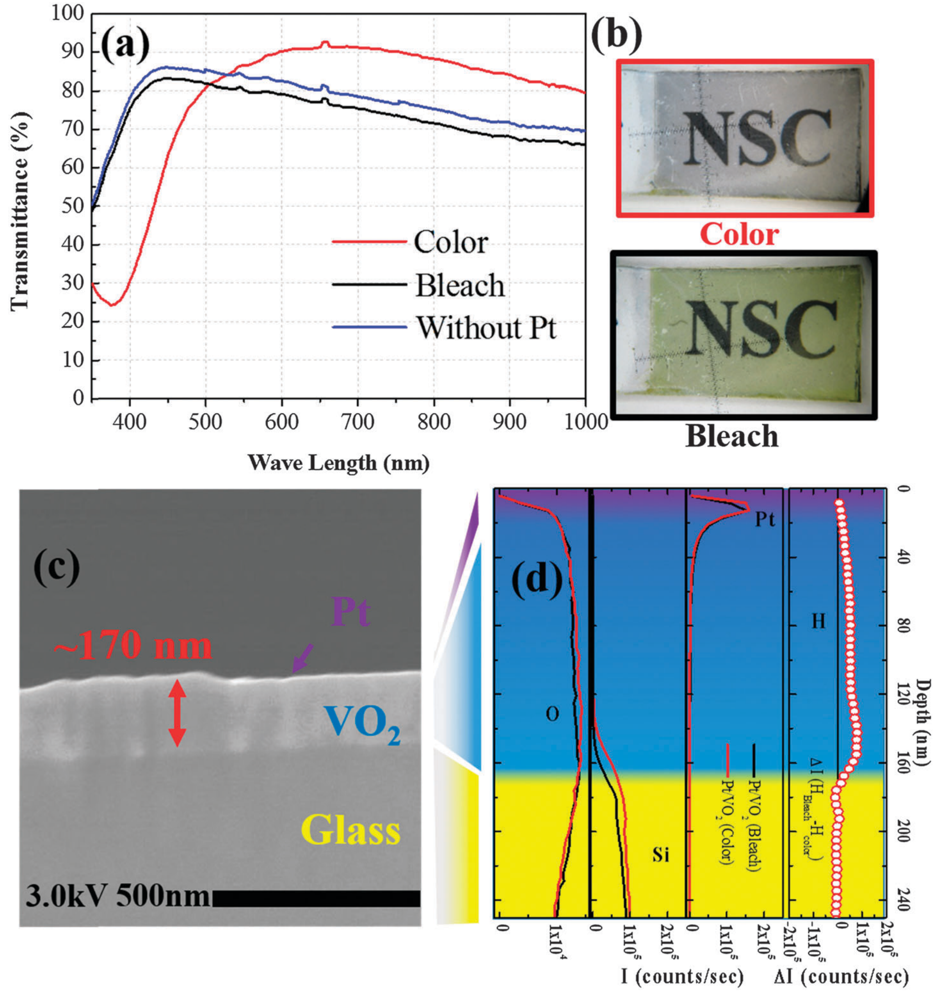

Fig. 1 (a) Transmission spectra of gasochromic Pt/VO_2 films. (b) Photograph of films in colored and bleached states. (c) Cross-sectional SEM images of Pt/VO_2 films. (d) Comparison of SIMS of the O, Si, Pt, and H depth profiles for bleached and colored films.

effect of the adsorption of H_2 on the film, Fig. 1(d) (right panel) displays the difference in the depth profile of hydrogen in the film in the bleached and colored states. Surface and substrate effects may cause the H concentration close to the surface and the substrate to differ from that in the middle of the film. According to the H profile in the middle region, the hydrogen concentration in the VO_2 is approximately constant. The concentration of hydrogen falls to zero at a depth in the substrate of 170–180 nm. This result indicates that in the gasochromic reaction, hydrogen ions are incorporated not only into the surface but also into the interior of the film, potentially causing structural distortions, as evidenced by subsequent structural characterizations. The coloration in VO_2 thin films is believed to be determined by electrons and so the electronic structure of such films must be examined.

V K-edge XAS is sensitive to the valence and local atomic environments of the absorbing element and is also influenced by constructive and destructive interferences (single and multiple scattering) by more distant neighbors around the central absorbing atoms – vanadium in this case, by the electronic many-body effects (such as quadrupolar transitions), and by changes in the medium- and long-range environments. Therefore, the V K-edge was measured herein and Fig. 2(a) shows the spectra of the sample before (black curve) and after (red curve) coloration, along with the valence states of the vanadium oxides as reference samples. The spectra of the V K-edge arise from the transitions from the V 1s core level to the 4p-derived final states, and the V 4p unoccupied state with multiple transitions are responsible for the main absorption features from 5483 to 5502 eV. The features in the bleached spectrum are similar to those of the spectrum of monoclinic VO_2, suggesting that the film herein exhibits a VO_2-like structure, as will be verified by the results of EXAFS, which are discussed below. The pre-peak of the V K-edge is well known to be a formally forbidden 1s–3d electronic transition, which is dipole-allowed if the full local O_h symmetry is reduced. Hence, an intense per-edge feature A_2 appears between 5466 and 5475 eV, owing to the hybridized band of O 2p–V 3d orbitals (quadruple-allowed transitions) *via* V 4sp and V 3d hybridization. The intensity of such a pre-peak increases from perfect octahedral symmetry (VO) to distorted octahedral VO_6 groups (V_2O_3 and VO_2) and further to the lower coordination of the distorted square-pyramidal VO_5 group (V_2O_5).[23]

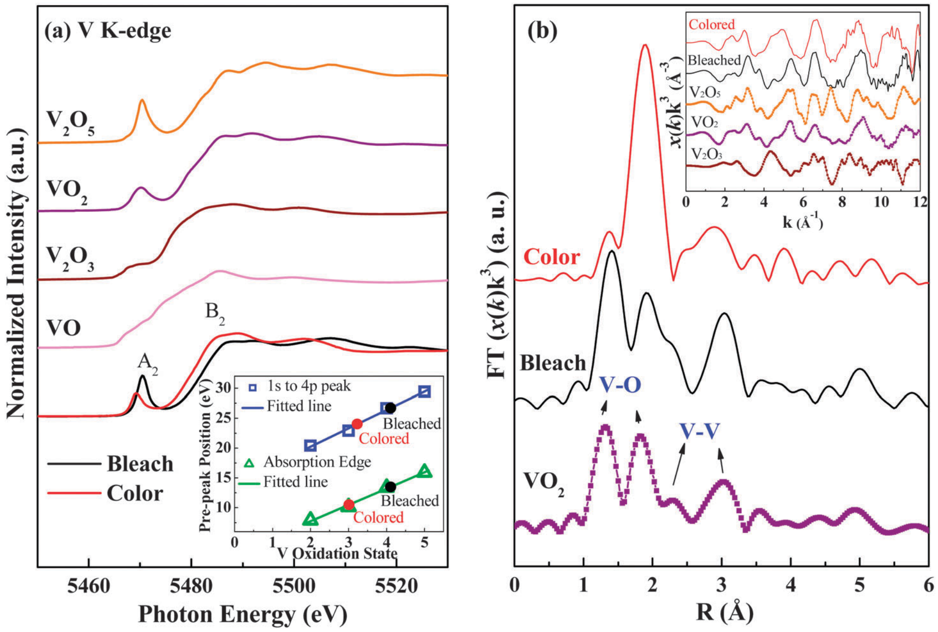

Fig. 2 (a) Normalized V K-edge XANES spectra of Pt/VO_2 films and various formal vanadium oxides. The inset plots least-square-fitted lines of the absorption edge and the 1s to 4p main peak. (b) Fourier transform (FT $x(k)k^3$) of EXAFS profiles of VO_2 and Pt/VO_2 films. The inset presents EXAFS oscillations of formal vanadium oxides and Pt/VO_2 films.

Accordingly, the intensity of the pre-peak region is strongly related to the local coordination symmetry. Pre-edge A_2 is less pronounced in the colored state than in the bleached state because the vertical asymmetry of the apical V–O bond becomes more symmetric in the colored state.

Not only is the intensity of the pre-peak of the film in the colored state lower, but also the energies of the pre-peak and the main absorption peak B_2 are lower. The energies of the absorption features are correlated with the vanadium valence state. Herein, two methods are adopted to estimate the charge state of vanadium in the film upon coloration,[23,24] as presented in the inset of Fig. 2(a). With reference to the results at the top of this inset, the valence state is obtained from the energy of the derivative curve of the absorption edge. The bottom displays the energy of the main peak that arises from the 1s to 4p absorption. The data in the inset in Fig. 2(a) are least-square-fitted with a slope (energy shift) of 2.7 eV per valence at the absorption edge and a slope of 3 eV for the 1s to 4p main peak. The slopes are consistent with the XAS measurements that were made by J. Wong *et al.*[23] The formal valence state of vanadium in the bleached film is about 4+ with the electronic configuration $3d^1$. Notably, the intensity of the pre-peak from the bleach film is higher than that from the powdered VO_2 (M), suggesting that the coordination symmetry of the bleached film is more distorted than that of powdered VO_2 (M). When the H ions are introduced, the electron enters into the d orbital and the valence of vanadium is changed from 4+ to 3+ in the colored state. Thus, the decrease of the unoccupied V 3d states is accompanied by a downshift in the edge position from the pre-edge of the V K-edge spectrum. This result is confirmed by the O K-edge, as will be discussed later in relation to Fig. 3.

Fig. 2(b) shows the Fourier transform modules of EXAFS profiles in real space to elucidate the local atomic structure of bleached and colored films. The inset of Fig. 2(b) presents the $x(k)$ oscillations of the bleached and colored states, and compares them with those of reference oxides V_2O_3, VO_2 and V_2O_5. The oscillations of the reference oxides are consistent with other reports.[24–27] The profile of oscillation in bleach is similar to that in powdered VO_2 (M), but the amplitudes differ. Accordingly, these materials have similar local structures but different coordination numbers. Upon coloration, the oscillation changes, implying that the structure of the film was modified. In Fig. 2(b), four distinct peaks in the Fourier transform curves of powdered VO_2 (M) are identified; the two peaks at 1.3 and 1.8 Å correspond to the chemical bonds of the V–O, and the other two at 2.3 and 3.0 Å are associated with different V–V bonds.[25–27] As is presented in the figure, the coordination symmetry of the bleached film is more distorted than that of powdered VO_2, and this fact is consistent with the results obtained from the pre-edge of the V K-edge. Exposure to H_2 substantially reduces the intensity of the first peak at 1.4 Å, and increases that of the second peak at 1.9 Å. The two split V–O peaks merge into a single peak, suggesting an increase in the symmetry of the VO_6 octahedra with all the V–O bond lengths being similar. This result implies that the structure is modified. This modification of the structure from monoclinic to rutile-like is consistent with the work of C. Wu *et al.*, who considered modulated electron–electron correlation effects.[25]

When the V–V distance is smaller than a critical distance (2.94 Å), the coupling interaction between 3d electrons has been suggested to cause itinerant electronic behavior.[28] In the reference VO_2 (M), the V–V pairs have both a short V–V (2.3 Å)

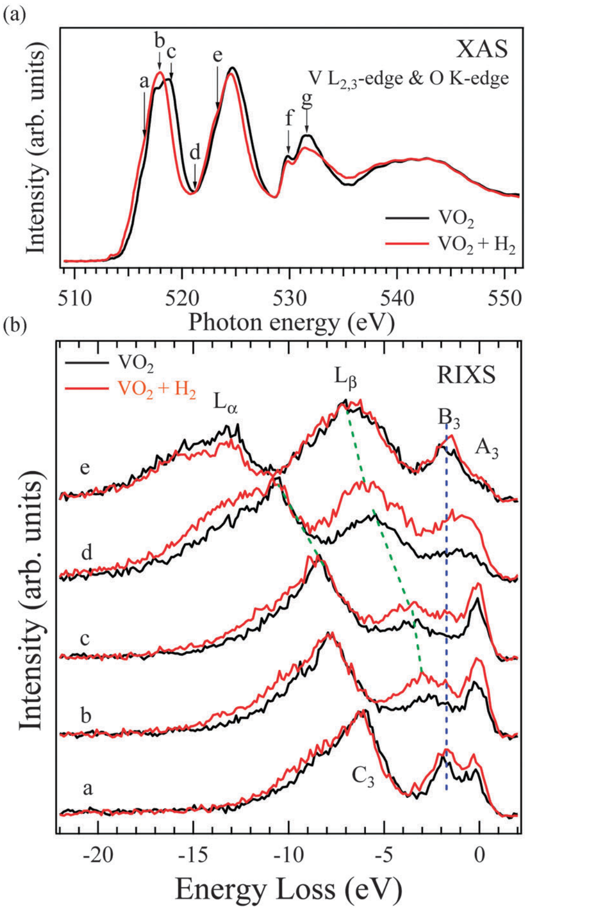

Fig. 3 (a) V $L_{2,3}$-edge and O K-edge XAS of films in bleached and colored states. (b) RIXS spectra on the energy loss scale obtained at excitation energies that are marked by arrows in XAS in (a).

bond and a long V–V (3.0 Å) bond. The long V–V length (3.0 Å) exceeds the critical distance, so the d-orbital electrons are only localized within the short V–V pairs, yielding the bleached state of VO_2. The hydric process reduces the long V–V bond length to 2.9 Å, which is less than the critical distance, enabling the delocalization of the d electrons among V atoms. This situation is very similar to that when VO_2 is at 340.8 K, and the fitted long V–V length is 2.90 Å, which causes VO_2 to exhibit metallic behavior.[25] When the hydrogen is incorporated into monoclinic-like VO_2, the modulation of the electron–electron correlation seems to change the monoclinic-like VO_2 to the rutile-like VO_2. The additional electrons in the vanadium–oxygen lattice frameworks stabilize the rutile-like VO_2 (R) phase by the hydric process at room temperature. Thus, whether the electron is localized and delocalized is important and the correlation of V 3d electrons may provide critical information.

Fig. 3(a) displays the V L- and O K-edge XAS spectra of bleached and colored films. The spin–orbital coupling splits the V 2p core hole level into the $2p_{3/2}$ and $2p_{1/2}$ levels, yielding V L_3 and V L_2 edges at around 518 and 525 eV, which arise from V $2p_{3/2} \rightarrow$ V 3d and V $2p_{1/2} \rightarrow$ V 3d transitions, respectively. Above the V L_2-edge is the O K-edge, which originates in the O 1s → O 2p transition. The double peak between 528 and 535 eV is attributed to the hybridization of the O 2p states with the V 3d t_{2g} and e_g states that are split by the crystal field. The broad structure at around 542 eV is generated by hybridization between O 2p states and V 4sp states.[29] Exposure to hydrogen chemically shifts the V $L_{2,3}$-edge to a lower energy and smears out the fine structures. The V L-edge XAS presents the partial density of states of the d orbital and the area under the absorption feature is proportional to the amount of the unoccupied d states. The area is determined by integration to be 3.5 and 3.3 for the films in the bleached and colored states. As is shown, in the monoclinic phase without incorporated H^+, the unoccupied d state is associated with a larger area than the colored film, implying fewer electrons in the d orbitals. Upon coloration with incorporated H^+, the area becomes smaller, indicating that more electrons have entered the d orbital. Accordingly, the probability of interaction between the d orbitals of nearest-neighboring vanadium atoms is increased and the electron–electron correlation effects along the infinite linear V–V chains are strengthened. This effect demonstrates the drop in the valence state of vanadium, which can be understood as being caused by a decrease in the attractive potential of the nucleus and a weakening of the repulsive Coulomb interaction of the core with the other electrons in the compound.

The change in the valence state is confirmed by the fact that the 3d t_{2g} state is filled so that the intensity at about 530 eV in the O K-edge is reduced upon reaction with H_2. Electrons may enter the 3d t_{2g} orbital, reducing the V oxidation state, accompanied by a downshift in the energy of the V $L_{2,3}$-edge. The e_g states at around 531 eV broadened perhaps by the modulation of structural symmetry, which influences the crystal-field effect.[30,31] Based on the concurrent advances in the atomic and electronic structures, both the structural modulation and the electron correlations that are caused by H_2 intercalation may be responsible for the color switching of VO_2. Hence, the d orbital should receive more attention since the spatial distributions of the electron clouds in the lattice before and after gasochromism differ. Therefore, before the gasochromic reaction, the local structure is monoclinic-like so electron clouds move in the zigzag direction locally; after the gasochromic reaction, the local structure is rutile-like so the electron clouds are along the V–V chains. The shrinking of the V–V distance causes sharing of d electrons among V atoms along the V–V chain and generates the electron–electron correlation. The localization/delocalization determines the electronic states.

To verify that H^+ incorporation indeed promotes the correlation of electrons, RIXS was utilized. RIXS is regarded as a useful tool for elucidating the inter-shell transition that is caused by charge transfer excitation and the inner-shell transition associated with d–d excitation in many transition metal oxides,[29,32] and, thereby, the correlation of electrons. Fig. 3(b) displays the RIXS spectra that were recorded using the various excitation energies that are specified in Fig. 3(a). To obtain the energy-loss spectra, the energy of the emitted photons in each spectrum is subtracted from the energy of the incoming photon (excitation energy). The spectra vary greatly with the excitation energy. Three processes – elastic scattering, inelastic scattering and normal fluorescence emission – contribute to the spectra. The elastic scattering (feature A_3) involves no energy loss, so the energy of the scattered photons equals that of the incoming photons. The excited feature B_3 at the lowest energy of approximately −1.6 eV is resonantly enhanced when the energy is tuned to the region of the main V L_3 peak (a–c). This feature is associated with the d–d excitation and is regarded as an indication of the strength of the correlation between the 3d electrons and the occupancy of the 3d orbital.[29,32–35] This energy-loss feature B_3 of the colored film has a greater intensity than that of the bleached film, suggesting that more electrons occupy the 3d orbital and participate in d–d excitation following coloration. The colored film exhibits more intense V 3d LPDOS, as revealed by the larger area, C_3, which disperses to lower energy as the excitation energy is increased, supporting the claim that gasochromism increases the number of electrons that occupy the 3d orbital and reduces the valence. A peak at a lower energy, close to that of d–d excitation, is attributed to the V L_β band (green dashed line).[29,32] In fact, the incorporation of H^+ ions into the lattice contributes additional electrons to the V–O system. The extra electrons in the V–O system strengthen the electron–electron correlation between the neighboring vanadium atoms in the linear V–V chains.

Fig. 4(a) shows the RIXS spectra that were obtained by excitation at the energies indicated by f and g, which, respectively, correspond to the t_{2g} and e_g bands in the O K-edge for the film both before and after the gasochromic reaction. Peak A_4 is shifted to a higher energy as the excitation energy is increased and is assigned to elastic scattering. Notably, a non-symmetric peak is obtained from the film in the bleached state. The appearance of a shoulder-like structure at about 526 eV is attributable to the non-equivalent oxygen site, which has been successfully demonstrated in high-Tc superconductors.[36] Thus, the absence of such a shoulder may suggest that the structure is more symmetrical upon coloration, supporting the result from the V K-edge, which reveals that the vertically asymmetric apical V–O bond is more symmetrical in the colored state than in the bleached state. The results are consistent with the EXAFS results that are shown in Fig. 2(b). Fig. 4(b) compares the RIXS spectra taken at energies a and g at the V L-edge and the O K-edge, respectively. The O 1s RIXS spectrum reveals an O 2p band at the lower energy of ∼−6 eV and the V 2p RIXS spectrum includes a V 3d band at a higher energy of ∼−5.5 eV. According to this comparison of both spectra on the energy loss scale, the O 2p and V 3d bands are strongly hybridized with each other. Owing to the strong O 2p–V 3d hybridization, the d–d excitation is also observed in the O RIXS spectrum, as indicated by the vertical line at 1.6 eV. The inset clearly demonstrates the enhancement of the d–d excitation in the film upon coloration. The band gaps were further estimated by comparing the XAS with the XES, as presented in the absorption–emission spectrum in Fig. 4(c). Based on the valence band maximum and the conduction band minimum, estimated by a standard method,[37] the band gap of bleach is about 0.7 eV, which is consistent with the band gap of VO_2.[11] The shift of the band gap can be determined by the first-order derivative of the absorption and emission spectra, as shown in the inset. The band gap is reduced upon coloration.

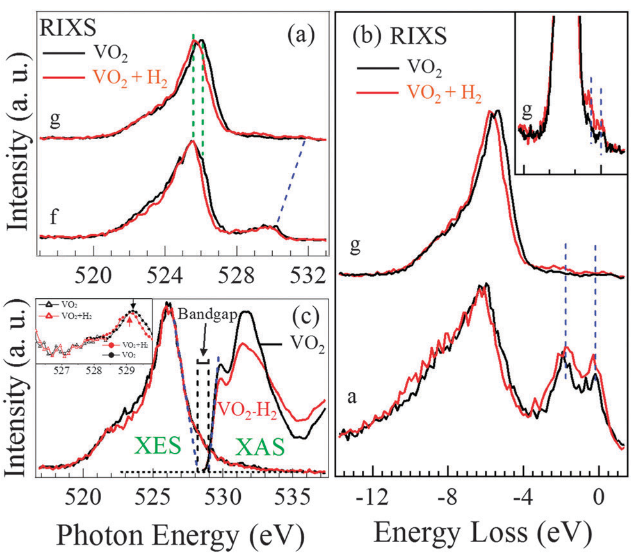

Fig. 4 (a) O 1s RIXS spectra. (b) Comparison of O 1s and V 2p RIXS spectra on the energy loss scale. The inset highlights V 3d LPDOS in O 1s RIXS spectra. (c) Bandgap obtained from absorption–emission spectra.

The regulation of the electron–electron correlation in VO_2 was recently identified as an effective way to control the carrier concentration selectively; such control is crucial to improve thermoelectric properties.[25] Gasochromism, another phenomenon with promising application, also arises from the electron–electron correlation. Monoclinic VO_2 (M) is the prototype material for understanding the correlation effect in solids,[25,28] in which the relationship between the correlation and the electronic structure has been extensively examined. As is well known, monoclinic VO_2 (M) (room temperature phase, <340 K) and rutile VO_2 (R) (non-ambient phase, >340 K) are typical states in a temperature-driven, fully reversible structural phase-transition process. Similarly, herein, the gasochromism of VO_2 depends strongly on the atomic/electronic structure and electronic correlations. Upon coloration, the shifting of vanadium atoms from VO_2 monoclinic-like (zigzag type) to rutile-like VO_2 (linear chains) causes the evolution from the localized to the delocalized d-orbital electron cloud.[25,38] In this respect, the orientational change of electron clouds affects the electronic state and the correlation of electrons upon lattice modulation. In fact, this electron–electron correlation even has a significant effect on the band gap of thermochromic VO_2, forming insulation or metallic states in monoclinic VO_2 (M) and rutile VO_2 (R), as reported by Wu *et al.*[25] The incorporation of hydrogen into VO_2 (R) can stabilize its metallic phase, even at room temperature. The hydrogen ions are believed to contribute additional electrons to the V–V chain strengthening the electron–electron correlation and stabilizing the metallic phase. Metallic VO_2 (R), insulating VO_2 (M) and the intermediate semiconducting phase can be obtained by controlling the hydrogen concentration in VO_2. Therefore, the electronic and optical properties, and therefore the band gap, can be tuned by varying the hydrogen concentration. This phenomenon provides an intriguing route for controlling the color of the gasochromic film by modulating the electron correlation. The variations in V–O and V–V pairs are found to play essential roles in the evolution of atomic/electronic structures, resulting in the gasochromic coloration of VO_2. The strong correlations among atomic spatial rearrangement, electronic structures, and transmittance support a cooperative mechanism of the gasochromic transition of VO_2. The above results establish a clear correlation between the dynamics of the lattice structure and electronic properties and suggest a potential pathway that gives rise to gasochromism.

Summary

VO_2 thin films for gasochromic application were fabricated by the sol–gel spin-coating technique. The geometric and electronic structures of the gasochromic VO_2 thin films following the hydric reaction were characterized by XAS and XES. This work reports for the first time the gasochromic phenomenon in VO_2. The spectroscopic results reveal that the bleached film has the local structure of monoclinic-like VO_2 with a V valence of close to 4+. Upon coloration, the structure becomes rutile-like VO_2 with a reduction of the valence state. Notably, VO_2 is known to be the M-phase at room temperature. The hydric VO_2 herein has the R-phase. This work describes a new physical insight in which the regulation of atomic and electronic structures in a material supports advances in the control of localized/delocalized electrons and, thereby, electron–electron correlation effects, potentially leading to the design of novel gasochromic materials.

Acknowledgements

This work is supported by the Ministry of Science and Technology (MOST) (formerly the National Science Council (NSC)) of Taiwan, under contracts no. MOST 101-212-M-213-004-MY3 and 102-2112-M-001-004-MY3.

References

1 C. G. Granqvist, *Sol. Energy Mater. Sol. Cells*, 2007, **91**, 1529–1598.
2 H. Zheng, J. Z. Ou, M. S. Strano, R. B. Kaner, A. Mitchell and K. Kalantar-zadeh, *Adv. Funct. Mater.*, 2011, **21**, 2175–2196.
3 P. Ngene, T. Radeva, M. Slaman, R. J. Westerwaal, H. Schreuders and B. Dam, *Adv. Funct. Mater.*, 2014, **24**, 2374–2382.
4 C. G. Granqvist, *Nat. Mater.*, 2006, **5**, 89–90.
5 V. Wittwer, M. Datz, J. Ell, A. Georg, W. Graf and G. Walze, *Sol. Energy Mater. Sol. Cells*, 2004, **84**, 305–314.
6 H. S. Choi, J. S. Ahn, J. H. Jung, T. W. Noh and D. H. Kim, *Phys. Rev. B: Condens. Matter Mater. Phys.*, 1996, **54**, 4621–4628.
7 T. Driscoll, J. Quinn, S. Klein, H. T. Kim, B. J. Kim, Y. V. Pershin, M. Di Ventra and D. N. Basov, *Appl. Phys. Lett.*, 2010, **97**, 093502.
8 D. Ruzmetov, S. D. Senanayake and S. Ramanathan, *Phys. Rev. B: Condens. Matter Mater. Phys.*, 2007, **75**, 195102.
9 M. S. Laad, L. Craco and E. Müller-Hartmann, *Phys. Rev. B: Condens. Matter Mater. Phys.*, 2006, **73**, 195120.
10 F. J. Morin, *Phys. Rev. Lett.*, 1959, **3**, 34–36.
11 C. N. Berglund and H. J. Guggenheim, *Phys. Rev.*, 1969, **185**, 1022–1033.
12 H. Kim, Y. Kim, K. S. Kim, H. Y. Jeong, A. R. Jang, S. H. Han, D. H. Yoon, K. S. Suh, H. S. Shin, T. Kim and W. S. Yang, *ACS Nano*, 2013, **7**, 5769–5776.
13 J. D. Zhou, Y. F. Gao, Z. T. Zhang, H. J. Luo, C. X. Cao, Z. Chen, L. Dai and X. L. Liu, *Sci. Rep.*, 2013, **3**, 3029.
14 J. B. Goodenough and H. Y.-P. Hong, *Phys. Rev. B: Solid State*, 1973, **8**, 1323–1331.
15 Y. Mruaoka and Z. Hiroi, *Appl. Phys. Lett.*, 2002, **80**, 583–585.
16 J. P. Pouget, H. Launois, J. P. O'Haenens, P. Merenda and T. M. Rice, *Phys. Rev. Lett.*, 1975, **35**, 873–875.
17 Y. F. Wu, L. L. Fan, S. M. Chen, S. Chen, C. W. Zou and Z. Y. Wu, *AIP Adv.*, 2013, **3**, 042132.
18 J. M. Booth and P. S. Casey, *Phys. Rev. Lett.*, 2009, **103**, 086402.
19 A. Kotani and S. Shin, *Rev. Mod. Phys.*, 2001, **73**, 203–246.
20 K. L. Tsang, C. H. Lee, Y. C. Jean, T. E. Dann, J. R. Chen, K. L. D'Amico and T. Oversluizen, *Rev. Sci. Instrum.*, 1995, **66**, 1812–1814.
21 T. Warwick, P. Heimann, D. Mossessian, W. McKinney and H. Padmore, *Rev. Sci. Instrum.*, 1995, **66**, 2037–2040.
22 J. Nordgren, G. Bray, S. Cramm, R. Nyholm, J. E. Rubensson and N. Wassdahl, *Rev. Sci. Instrum.*, 1989, **60**, 1690–1696.
23 J. Wong, F. W. Lytle, R. P. Messmer and D. H. Maylotte, *Phys. Rev. B: Condens. Matter Mater. Phys.*, 1984, **30**, 5596–5610.
24 F. Haaß, A. H. Adams, T. Buhrmester, G. Schimanke, M. Martin and H. Fuess, *Phys. Chem. Chem. Phys.*, 2003, **5**, 4317–4324.
25 C. Z. Wu, F. Feng, J. Feng, J. Dai, L. L. Peng, J. Y. Zhao, J. L. Yang, C. Si, Z. Y. Wu and Y. Xie, *J. Am. Chem. Soc.*, 2011, **133**, 13798–13801.
26 C. Marini, S. Pascarelli, O. Mathon, B. Joseph, L. Malavasi and P. Postorino, *EPL*, 2013, **102**, 66004.
27 X. G. Tan, T. Yao, R. Long, Z. H. Sun, Y. J. Feng, H. Cheng, X. Yuan, W. Q. Zhang, Q. H. Liu, C. Z. Wu, Y. Xie and S. Q. Wei, *Sci. Rep.*, 2012, **2**, 466.
28 T. Yao, X. D. Zhang, Z. H. Sun, S. J. Liu, Y. Y. Huang, Y. Xie, C. Z. Wu, X. Yuan, W. Q. Zhang, Z. Y. Wu, G. Q. Pan, F. C. Hu, L. H. Wu, Q. H. Liu and S. Q. Wei, *Phys. Rev. Lett.*, 2010, **105**, 226405.
29 T. Schmitt, L.-C. Duda, M. Matsubara, M. Mattesini, M. Klemm, A. Augustsson, J.-H. Guo, T. Uozumi, S. Horn, R. Ahuja, A. Kotani and J. Nordgren, *Phys. Rev. B: Condens. Matter Mater. Phys.*, 2004, **69**, 125103.
30 G. P. Zhang, G. T. Woods, E. L. Shirley, T. A. Callcott, L. Lin, G. S. Chang, B. C. Sales, D. Mandrus and J. He, *Phys. Rev. B: Condens. Matter Mater. Phys.*, 2002, **65**, 165107.
31 W. L. Jang, Y. M. Lu, C. L. Chen, Y. R. Lu, C. L. Dong, P. H. Hsieh, W. S. Hwang, J. L. Chen, J. M. Chen, T. S. Chan,

J. F. Lee and W. C. Chou, *Phys. Chem. Chem. Phys.*, 2014, **16**, 4699–4708.
32 T. Schmitt, L.-C. Duda, M. Matsubara, A. Augustsson, F. Trif, J.-H. Guo, L. Gridneva, T. Uozumi, A. Kotani and J. Nordgren, *J. Alloys Compd.*, 2004, **362**, 143–150.
33 S. Shin, A. Agui, M. Watanabe, M. Fujisawa, Y. Tezuka and T. Ishii, *J. Electron Spectrosc. Relat. Phenom.*, 1996, **79**, 125–130.
34 S. Shin, M. Fujisawa, H. Ishii, Y. Harada, M. Watanabe, M. M. Grush, T. A. Callcott, R. C. C. Perera, E. Z. Kurmaev, A. Moewes, R. Winarski, S. Stadler and D. L. Ederer, *J. Electron Spectrosc. Relat. Phenom.*, 1998, **92**, 197–205.
35 L. Braicovich, G. Ghiringhelli, L. H. Tjeng, V. Bisogni, C. Dallera, A. Piazzalunga, W. Reichelt and N. B. Brookes, *Phys. Rev. B: Condens. Matter Mater. Phys.*, 2007, **76**, 125105.
36 J.-H. Guo, S. M. Butorin, N. Wassdahl, J. Nordgren, P. Berastegut and L.-G. Johansson, *Phys. Rev. B: Condens. Matter Mater. Phys.*, 2000, **61**, 9140–9144.
37 C. L. Dong, S. S. Chen, J. W. Chiou, Y. Y. Chen, J. H. Guo, H. F. Cheng, I. N. Lin and C. L. Chang, *Diamond Relat. Mater.*, 2008, **17**, 1150–1153.
38 M. S. Grinolds, A. Lobasstov, J. Weissenrieder and A. H. Zewail, *Proc. Natl. Acad. Sci. U. S. A.*, 2006, **103**, 18427–18431.